CRYSTAL GROWTH & DESIGN
2004
VOL. 4, NO. 6
1371−1375

Dextran-Controlled Crystallization of Silver Microcrystals with Novel Morphologies

Jinhu Yang, Limin Qi,* Dongbai Zhang, Jiming Ma, and Humin Cheng

State Key Laboratory for Structural Chemistry of Unstable and Stable Species, College of Chemistry, Peking University, Beijing 100871, People's Republic of China

Received June 2, 2004

ABSTRACT: The controlled synthesis of silver microcrystals with novel morphologies, such as solid or multiholed single crystalline disks, flowerlike aggregates consisting of platelike petals, and dendritic crystals consisting of wide leaves, was realized by using the polysaccharide dextran as a crystal growth modifier. The effects of dextran nature, dextran concentration, temperature, and solvent on the morphology of the silver crystals were investigated, and the obtained products were characterized by scanning electron microscopy, transmission electron microscopy, and X-ray diffraction. While the nonionic dextran showed little effect on the silver crystallization, the anionic dextran sulfate exhibited a significant influence on the morphology of the silver crystals. Silver microdisks with solid or multiholed structures were facilely obtained in water at a high dextran sulfate concentration (100 g L^{-1}). With the aid of formamide, silver microdisks with thicknesses as thin as 50 nm can be easily obtained at a relatively low dextran sulfate concentration (10 g L^{-1}).

Introduction

Systematically manipulating the morphology and architecture of inorganic crystals at microscale and nanoscale levels is a significant challenge, which is increasingly concerning due to their strong influence on materials properties.[1−4] Inspired by the biomineralization process where biomacromolecules control the nucleaction and growth of inorganic structures resulting in the formation of biominerals that show complex forms or hierarchical architectures, synthetic polymers[5−8] as well as biomacromolecules[9,10] have been used as effective crystal growth modifiers for the morphological control of inorganic minerals. Recently, the morphological control of silver crystals has been the focus of intensive research due to their potential applications related to their unique optical, electronic, and catalytic properties, which are largely determined by their shape and structure. For example, a variety of solution synthetic methods have been developed for the shape-controlled synthesis of nanoscale silver cubes,[3] rods/wires,[11] belts,[12] plates,[4,12−14] and dendrites.[15] However, there is only limited success in the morphological control of silver crystals at submicrometer or micrometer scales although large colloidal silver particles may find important applications in catalysis, sensing, surface-enhanced Raman spectroscopy (SERS), and photonic crystals.[16−18] It is noteworthy that soluble biomacromolecules such as peptides have been successfully used for the biomimetic synthesis and patterning of silver nanoparticles.[19] Nevertheless, the use of biorelated macromolecules other than proteins for the shape-controlled synthesis of silver crystals remains to be explored.

Dextran, which can be conveniently modified with charged substituents, is a water soluble polysaccharide composed of repeated monomeric glucose units with a predominance of α-1,6-linkages. Recently, dextran gels have been used as soft templates for the novel synthesis of metallic and metal oxide sponges.[20] On the other hand, various ionic and nonionic dextrans have been used as additives to investigate the effects of polymers on the crystallization of metal hydroxides and carbonates, and significant effects have been observed for the anionic derivative of dextran, dextran sulfate.[21] In the present work, the shape-controlled synthesis of micrometer-sized silver crystals with novel morphologies was realized simply by the reduction of Ag^+ ions with ascorbic acid in aqueous solutions of nonionic and anionic dextrans. The effects of dextran nature, dextran concentration, temperature, and solvent on the silver crystallization were investigated in detail.

Experimental Section

Materials. The nonionic dextran (Dex-40, MW 40000) and the anionic dextran, dextran sulfate (DexS-40, MW 40000), were purchased from Roth (Germany). All of the other chemical reagents were of analytical grade, and the water used was deionized.

Crystallization of Silver. In a typical synthesis of silver crystals, a certain amount (e.g., 1 g) of Dex-40 or DexS-40, 1 mL of 0.2 M ascorbic acid ($C_6H_8O_6$) solution, and 8 mL of water were mixed first. After DexS-40 was dissolved completely and the solution was thermostated at either 20 or 60 °C, 1 mL of 0.2 M $AgNO_3$ solution was added under vigorous stirring, giving a turbid solution with a final reactant concentration of 20 mM. Then, the solution was aged at the constant temperature under static conditions for 24 h, resulting in a gray precipitate, which was then collected by centrifugation. For the study of the solvent effect, the silver crystallization in the presence of DexS-40 was also conducted in mixed water−formamide solvents at 20 °C. The experimental procedure was similar to the one described for the silver crystallization in water except that mixed solutions of water and formamide were used as the mixed solvents and a lower reactant concentration (2 mM) was adopted to avoid the uncontrolled crystallization of the silver crystals. Our preliminary experimental results have shown that the precipitation process was usually so quick that our attempts to capture the initial state of the particles after mixing have failed and that the optical properties of the silver particles can hardly be measured in

* To whom correspondence should be addressed. E-mail: liminqi@chem.pku.edu.cn.

10.1021/cg049823g CCC: $27.50
Published on Web 09/03/2004

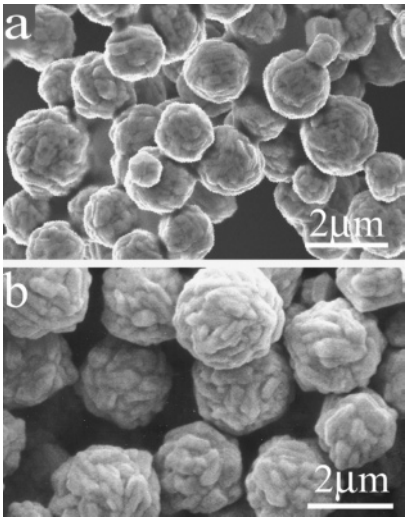

Figure 1. SEM images of Ag crystals formed at 20 (a) and 60 °C (b) in the absence of dextrans. [$AgNO_3$] = 20 mM.

solution as the quickly formed micrometer-sized particles are too large to transmit light.

Characterization. Scanning electron microscopy (SEM) measurements were performed with an Amray 1910FE microscope operated at 10 kV, and transmission electron microscopy (TEM) observations were conducted on a JEOL JEM-200CX microscope operated at 160 kV. Powder X-ray diffraction (XRD) patterns were recorded on a Rigaku Dmax-2000 diffractometer with Cu Kα radiation.

Results and Discussion

Silver ions were reduced to metal silver by ascorbic acid ($C_6H_8O_6$) according to the following reaction:[16]

$$C_6H_8O_6 + 2Ag^+ \rightarrow 2Ag + C_6H_6O_6 + 2H^+$$

Figure 1 shows typical SEM images of the products formed in the absence of dextrans, which suggests that spherical silver particles exhibiting rough surfaces were obtained at both 20 and 60 °C although the particles obtained at 60 °C (1.8−3.8 μm) were somewhat larger than the particles obtained at 20 °C (0.8−2.0 μm). When the nonionic Dex-40 was present in the solution with a concentration of 10 g L^{-1}, similar silver spheres (~3 μm) were generated at 20 °C (Figure 2a), indicating a relatively weak, nonspecific interaction between the nonionic dextran and the silver species, which was in good agreement with the previous observation of the weak effect of nonionic dextrans on the formation of minerals.[21] It was noted that the obtained particles showed considerably coarser surfaces, which could partly result from the higher viscosity due to the presence of Dex-40. As the temperature was increased to 60 °C, the surfaces of the silver spheres became much more rugged and the final silver particles showed a multiarmed or branching morphology (Figure 2b), which may be caused by the accelerated diffusion at elevated temperature.

In contrast to the nonionic dextran, the anionic dextran sulfate showed remarkable effects on the crystallization of silver in the solution. Figure 3 presents typical SEM images of silver crystals formed at 20 °C in DexS-40 solutions with varied concentrations. As shown in Figure 3a, spherical, dense, branching aggregates (2−3 μm) consisting of irregularly aligned polyhedral crystals were produced at a Dexs-40 concentration of 1 g L^{-1}. When the DexS-40 concentration was increased to 10 g L^{-1}, well-defined flowerlike aggregates (2−3 μm) consisting of flat hexagonal petals were obtained (Figure 3b). It indicated that the branching rate or packing density of the silver aggregates was decreased with increasing Dexs-40 concentration possibly due to the enhanced adsorption of DexS-40 on specific silver crystal surfaces. If the DexS-40 concentration was further increased to 100 g L^{-1}, well-separated silver microdisks about 2−4 μm in diameter (Figure 3c) and 80−120 nm in thickness (Figure 3d) were generated. The disks showed relatively flat surfaces and irregularly curved-in edges with nearly circle-like outlines.

The unique silver microdisks were further characterized to determine their crystal direction. As shown in Figure 4a, the XRD pattern showed sharp reflections corresponding to the face-centered cubic (fcc) structure of metallic silver with the (111) reflection intensified

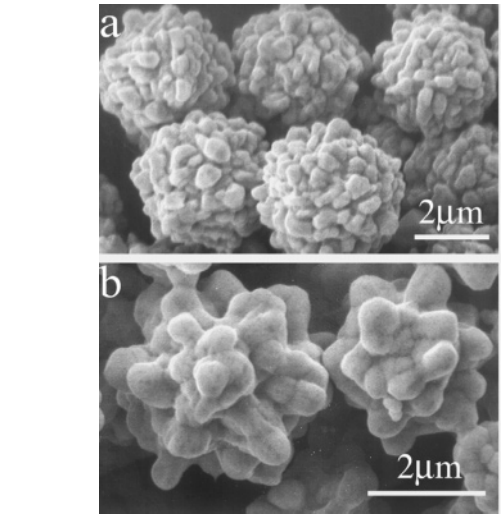

Figure 2. SEM images of Ag crystals formed at 20 (a) and 60 °C (b) in the presence of nonionic Dex-40. [$AgNO_3$] = 20 mM, and [Dex-40] = 10 g L^{-1}.

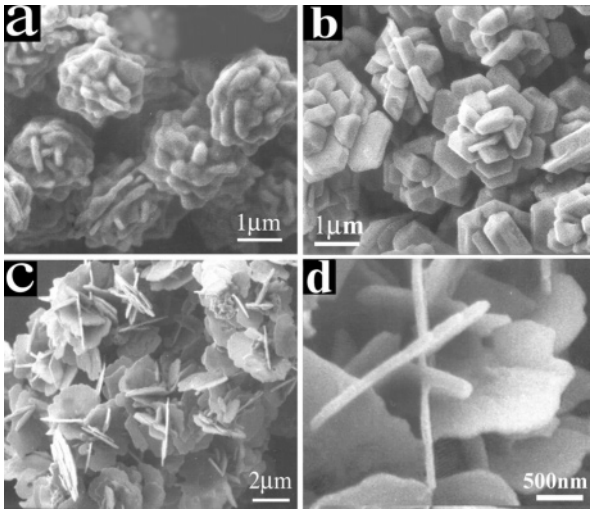

Figure 3. SEM images of Ag crystals formed in the presence of anionic DexS-40 at 20 °C. [$AgNO_3$] = 20 mM. [DexS-40]: (a) 1, (b) 10, and (c,d) 100 g L^{-1}.

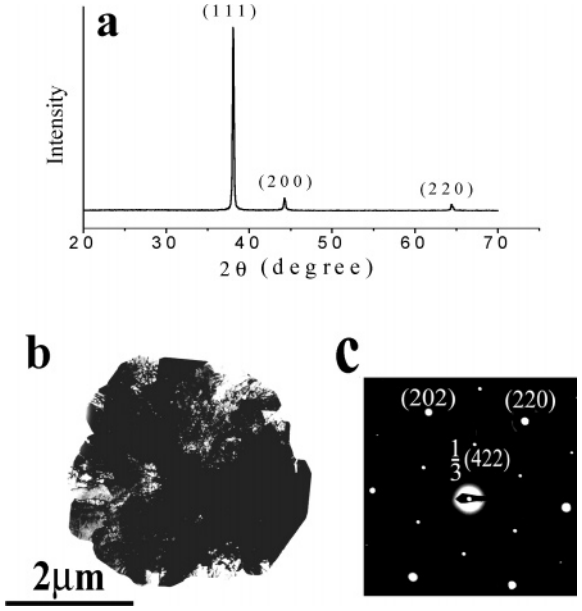

Figure 4. XRD pattern (a), TEM image (b), and ED pattern (c) of Ag microdisks formed in the presence of anionic DexS-40 at 20 °C. [$AgNO_3$] = 20 mM, and [DexS-40] = 100 g L^{-1}.

considerably, indicating that the disks were made of pure silver and their top face plane was the (111) plane. Figure 4b shows a typical TEM image of a silver disk about 4 μm in diameter, which suggested that the disk was not perfectly rounded, in good agreement with the SEM observation. The ED pattern of the disk (Figure 4c), which showed a hexagonal symmetry, exhibited a set of sharp spots with a spacing of 1.44 Å corresponding to the {220} reflections and an additional set of weak spots with a spacing of 2.50 Å corresponding to the (1/3){422} reflections.[4a,12,14b] This result suggested that the silver disk was a fcc single crystal with its top face bounded by the {111} planes, which is a very common structural configuration in platelike silver crystals such as Ag nanoprisms or nanodisks.[4,12−14] To the best of our knowledge, this is the first solution synthesis of micrometer-sized, platelike silver single crystals, which may find potential applications, e.g., as an efficient SERS substrate.

It is worth noting that Fukuyo and Imai have produced similar flowerlike silver aggregates consisting of platelike petals by the reduction of $AgNO_3$ with ascorbic acid at relatively high reactant concentrations without any additives although they have not obtained well-separated thin plates as in the present case.[18] As documented in the literature, the (111) plane of silver may possess the lowest surface energy, and the adsorption of suitable additives, such as citrate,[12,14f] cetyltrimethylammonium bromide (CTAB),[13b,14d,e] and silver-binding peptides,[19] on this plane may further lower the surface energy and stabilize the silver plates with the (111) plane as the basal plane. At relatively high concentrations of ascorbic acid (e.g., larger than 0.4 M), ascorbate anions could play roles both as a reducing agent and as a capping ligand in the absence of external additives just as the roles played by citrate anions in the synthesis of silver nanodisks in solution,[14f] which resulted in the formation of the flowerlike aggregates consisting of silver plates without additives. However, the ascorbate anions may be just a rather weak capping reagent so that well-separated silver plates with a nanometer-sized thickness were not obtained even at very high ascorbic acid concentrations (~2 M)[18] and only spherical particles (Figure 1) were produced at the relatively low ascorbic acid concentration (0.02 M) in the control experiment of this work. These results also indicate that ascorbic acid as well as its oxidation product have not contributed considerably to the formation of the current silver disks at the selected ascorbic acid concentration even though they are often considered as strong stabilizers by themselves. Therefore, it is highly possible that the preferential adsorption of DexS-40 on the (111) plane of Ag crystals played an important role in stabilizing this plane, leading to the formation of the silver microdisks with a top face of the (111) plane. As compared with the flowerlike aggregates obtained at lower DexS-40 concentrations, the silver microdisks obtained at the high DexS-40 concentration (100 g L^{-1}) may result from enhanced adsorption of DexS-40 on the (111) plane that effectively prevented the crystal aggregation. It is noted that only spherical aggregates of silver crystals (Figure 2a) were obtained when the reaction was conducted in the presence of the nonionic Dex-40 under otherwise similar conditions. This result could be rationalized by considering that the anionic sulfate groups of DexS-40 interacted strongly with Ag^+ ions and silver crystal surfaces, leading to a strong tendency of adsorption on the (111) plane, whereas the nonionic Dex-40 did not interact strongly with inorganic species, thereby providing no considerable control over the growth of silver crystals. However, it remains unclear why the sulfated polymer DexS-40 was preferentially adsorbed on the (111) plane of Ag crystals. In recent work, Au nanoplates with a top face of the (111) plane were prepared in the presence of a block copolymer containing hexacyclen and the molecular modeling results suggested that a perfect match of the hexacyclen part to the hexagons on the Au (111) face could lead to the preferential adsorption of the polymer to the (111) plane.[22] It may be argued that a similar lattice match exists between the DexS-40 and the Ag (111) plane in the present case; nevertheless, it is difficult to find such a structural match since the polymer chain is actually very flexible in solution, which is quite different from the relatively rigid structure of the hexacyclen. Moreover, the observed preferential adsorption of various low molecular weight additives inluding citrate,[12,14f] CTAB,[13b,14d,e] and peptides[19] on the Ag (111) plane indicates that effects other than structural match may be essential for the selective adsorption, which is certainly a subject worthy of further study.

It was observed that the morphology of the silver crystals obtained in the presence of DexS-40 was significantly influenced by temperature. As shown in Figure 5, silver crystals exhibiting unusual morphologies were formed when the temperature was increased to 60 °C. At a low DexS-40 concentration (i.e., 1 g L^{-1}), dendritic silver crystals larger than 10 μm were produced (Figure 5a), indicating a morphology change from a dense branching form (Figure 3a) to a dendritic form with increasing temperature. It has been documented that crystal morphologies depend on the correlation between the driving force of crystallization and the diffusion of reactants.[23] For example, faster diffusion

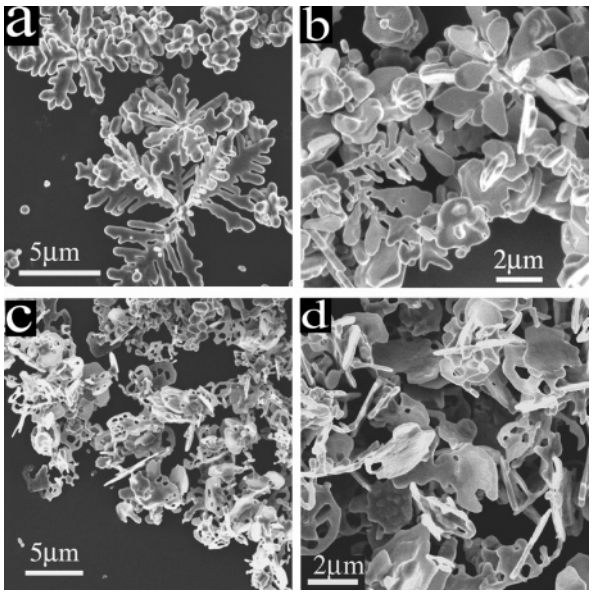

Figure 5. SEM images of Ag crystals formed in the presence of anionic DexS-40 at 60 °C. [$AgNO_3$] = 20 mM. [DexS-40]: (a) 1, (b) 10, and (c,d) 100 g L^{-1}.

would favor a morphology transition from a dense branching form to a dendritic form. In the current situation, accelerated diffusion at elevated temperature would contribute to the observed morphology transition of silver crystals. When the DexS-40 concentration was increased to 10 g L^{-1}, dendritic crystals consisting of wide leaves were produced (Figure 5b), which indicated a more pronounced adsorption of DexS-40 on the (111) plane of silver crystals, implying a tendency of transition from aggregated rods to separated plates. If the DexS-40 concentration was further increased to 100 g L^{-1}, unusual multiholed microdisks were generated (Figure 5c,d), which were also revealed to be single crystals with a top face of the (111) plane by the corresponding TEM study. It was proposed that at this temperature the initial reduction reaction and silver crystallization proceeded quite fast; hence, a large amount of DexS-40 molecules could be quickly wrapped within crystallizing silver disks due to the high DexS-40 concentration. The wrapped DexS-40 was dissolved gradually with time, and the holes appeared within the disks finally. As the hole sizes normally range from several tens of nanometers to ~1 μm, much larger than the size of a condensed single polysaccharide, it is highly possible that DexS-40 aggregates instead of a single DexS-40 molecule when wrapped within one hole.

It has been documented that the solvent can significantly influence the formation of silver particles since the solvent may show specific interaction with Ag^+ ions and affect physical properties of the reaction medium, such as the viscosity and the dielectric constant.[24,25] Formamide was selected as a cosolvent for the investigation of the solvent effect on the silver crystallization at 20 °C in the presence of anionic DexS-40 (10 g L^{-1}). Figure 6 displays typical SEM and TEM images of silver crystals formed at a reactant concentration of 2 mM in the mixed water−formamide solvents with varied formamide contents. As shown in Figure 6a, hexagonal plates, which were ~1 μm in size and ~0.4 μm in thickness and exhibited uneven top surfaces with

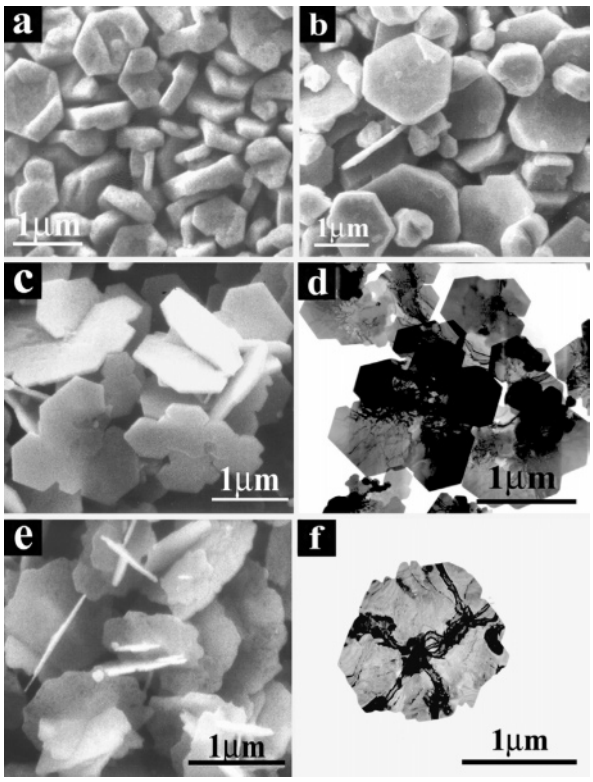

Figure 6. SEM (a−c,e) and TEM (d,f) images of Ag microdisks formed in mixed water−formamide solvents in the presence of anionic DexS-40 at 20 °C. [$AgNO_3$] = 2 mM, and [DexS-40] = 10 g L^{-1}. Formamide content (v %): (a) 0, (b) 10, (c,d) 50, and (e,f) 98.

concave portions, were produced in the absence of formamide. As compared with the flowerlike aggregates with hexagonal petals (Figure 3b) obtained at an identical DexS-40 concentration but a higher reactant concentration (20 mM), the current hexagonal plates were well-separated, indicating that a higher molar ratio of DexS-40 with respect to the reactants would prevent aggregation between individual hexagonal plates. When formamide was present with a volume content of 10%, hexagonal plates with relatively smooth top surfaces and a smaller thickness (~0.15 μm) were produced (Figure 6b). When the formamide content was increased to 50%, polygonal silver plates, which had a thickness about 80 nm and apparently consisted of several primary hexagonal plates, were obtained (Figure 6c,d). When the formamide content was further increased to 98%, nearly rounded silver disks with a diameter ~1 μm and a thickness as thin as 50 nm were generated (Figure 6e,f). The bandlike patterns shown on the surface of the nanodisk in Figure 6f could be attributed to differences of electron density on the microscopic scale. It is worth noting that the ED patterns related with Figure 6d,f were essentially the same as the ED pattern shown in Figure 4c, indicating that the present hexagonal plates and rounded disks were actually single crystals of silver with a top face of the (111) plane, similar to the silver disks (Figure 3c,d) obtained in water but at a much higher DexS-40 concentration (100 g L^{-1}). This result suggested that with increasing formamide content, the facetted edges of hexagonal plates became obscure and their thickness decreased gradually. Therefore, it provided a useful method to

obtain well-separated silver microdisks with a thickness less than 100 nm at a relatively low DexS-40 concentration (10 g L^{-1}) with the aid of formamide. There are two possible reasons for the promoted block of the (111) plane of the silver crystal in the presence of formamide. First, formamide could directly adsorb on the (111) plane of silver crystal due to its complexing ability with silver ions. Alternatively, formamide could considerably promote the interaction between DexS-40 and silver crystals due to the low solubility of DexS-40 in formamide.

Conclusion

Silver microcrystals showing a variety of novel morphologies were prepared readily by dextran-controlled crystallization. While the nonionic dextran showed a relatively weak effect on the silver crystallization, the anionic dextran sulfate exhibited a significant influence on the morphology of the silver crystals. It was found that the dextran sulfate concentration, temperature, and the solvent were the key factors in determining the final crystal morphology. Unique silver microdisks with solid or multiholed structures, which may find promising applications, were obtained in water at a high dextran sulfate concentration. Silver microdisks with thicknesses as thin as 50 nm can be obtained at a relatively low dextran sulfate concentration with the aid of formamide. This result may provide a facile, biomimetic route to the shape-controlled synthesis of metal crystals.

Acknowledgment. Financial support from NSFC (20325312, 20233010), FANEDD (200020), is gratefully acknowledged.

References

(1) (a) Mann, S. *Angew. Chem., Int. Ed*. **2000**, *39*, 3392. (b) Cölfen, H.; Mann, S. *Angew. Chem., Int. Ed*. **2003**, *42*, 2350.
(2) Peng, X.; Manna, L.; Yang, W.; Wickham, J.; Scher, E.; Kadavanich, A.; Alivisatos, A. P. *Nature* **2000**, *404*, 59.
(3) Sun, Y.; Xia, Y. *Science* **2002**, *298*, 2176.
(4) (a) Jin, R.; Cao, Y.; Mirkin, C. A.; Kelly, K. L.; Schatz, G. C.; Zheng, J. G. *Science* **2001**, *294*, 1901. (b) Jin, R.; Cao, Y.; Hao, E.; Metraux, G. S.; Schatz, G. C.; Mirkin, C. A. *Nature* **2003**, *425*, 487.
(5) (a) Qi, L.; Cölfen, H.; Antonietti, M. *Angew. Chem., Int. Ed.* **2000**, *39*, 604. (b) Qi, L.; Cölfen, H.; Antonietti, M.; Li, M.; Hopwood, J. D.; Ashley, A. J.; Mann, S. *Chem. Eur. J*. **2001**, *7*, 3526. (c) Cölfen, H.; Qi, L. *Chem. Eur. J*. **2001**, *7*, 106. (d) Zhang, D.; Qi, L.; Ma, J.; Cheng, H. *Chem. Mater*. **2002**, *14*, 2450.
(6) (a) Yu, S.-H.; Antonietti, M.; Cölfen H.; Giersig, M. *Angew. Chem., Int. Ed.* **2002**, *41*, 2356. (b) Yu, S.-H.; Cölfen H.; Antonietti, M. *Chem. Eur. J*. **2002**, *8*, 2937. (c) Yu, S.-H.; Antonietti, M.; Cölfen H.; Hartmann, J. *Nano Lett.* **2003**, *3*, 379. (d) Yu, S.-H.; Cölfen H.; Antonietti, M. *J. Phys. Chem. B* **2003**, *107*, 7396.
(7) (a) Naka, K.; Tanaka, Y.; Chujo, Y.; Ito, Y. *Chem. Commun.* **1999**, 1931. (b) Naka, K.; Tanaka, Y.; Chujo, Y. *Langmuir* **2002**, *18*, 3655. (c) Donners, J.; Heywood, B. R.; Meijer, E.; Nolte, R.; Roman, C.; Schenning, A.; Sommerdijk, N. *Chem. Commun.* **2000**, 1937. (d) Donners, J.; Heywood, B. R.; Meijer, E.; Nolte, R.; Sommerdijk, N. *Chem. Eur. J*. **2002**, *8*, 2561.
(8) (a) Sugawara, A.; Kato, T. *Chem. Commun.* **2000**, 487. (b) Park, H. K.; Lee, I.; Kim, K. *Chem. Commun.* **2004**, 24.
(9) (a) Belcher, A. M.; Wu, X. H.; Christensen, R. J.; Hansma, P. K.; Stucky, G. D.; Morse, D. E. *Nature* **1996**, *381*, 56. (b) Falini, G.; Albeck, S.; Weiner, S.; Addadi, L. *Science* **1996**, *271*, 67. (c) Aizenberg, J.; Lambert, G.; Weiner, S.; Addaddi, L. *J. Am. Chem. Soc.* **2002**, *124*, 32.
(10) Rautaray, D.; Ahmad, A.; Sastry, M. *J. Am. Chem. Soc.* **2003**, *125*, 14656.
(11) (a) Sun, Y.; Xia, Y. *Adv. Mater.* **2002**, *14*, 833. (b) Sun, Y.; Mayers, B.; Herricks T.; Xia, Y. *Nano Lett.* **2003**, *3*, 955. (c) Jana, N. R.; Gearheart, L.; Murphy, C. J. *Chem. Commun.* **2001**, 617. (d) Caswell, K. K.; Bender, C. M.; Murphy, C. J. *Nano Lett.* **2003**, *3*, 667. (e) Chimentao, R. J.; Kirm, I.; Medina, F.; Rodriguez, X.; Cesteros, Y.; Salagre, P.; Sueiras, J. E. *Chem. Commun.* **2004**, 846. (f) Zhang, D.; Qi, L.; Yang, J.; Ma, J.; Cheng, H.; Huang, L. *Chem. Mater.* **2004**, *16*, 872.
(12) Sun, Y.; Mayers, B.; Xia, Y. *Nano Lett.* **2003**, *3*, 675.
(13) (a) Pastoriza-Santos, I.; Liz-Marzan, L. M. *Nano Lett.* **2002**, *2*, 903. (b) Chen, S.; Carroll, D. L. *Nano Lett.* **2002**, *2*, 1003.
(14) (a) Hao, E.; Kelly, K. L.; Hupp, J. T.; Schatz, G. C. *J. Am. Chem. Soc.* **2002**, *124*, 15182. (b) Mailard, M.; Giorgio, S.; Pileni, M. P. *Adv. Mater.* **2002**, *14*, 1084. (c) Mailard, M.; Giorgio, S.; Pileni, M. P. *J. Phys. Chem. B* **2003**, *107*, 2466. (d) Chen, S.; Fan, Z.; Carroll, D. L. *J. Phys. Chem. B* **2002**, *106*, 10777. (e) Chen, S.; Carroll, D. L. *J. Phys. Chem. B* **2004**, *108*, 5500. (f) Maillar, M.; Huang, P.; Brus, L. *Nano Lett.* **2003**, *3*, 1611.
(15) (a) Xiao, J.; Xie, Y.; Tang, R.; Chen, M.; Tian, X. *Adv. Mater.* **2001**, *13*, 1887. (b) Wang, X.; Naka, K.; Itoh, H.; Park, S.; Chujo, Y. *Chem. Commun.* **2002**, 1300. (c) Wei, G.; Nan, C.-W.; Deng, Y.; Lin, Y.-H. *Chem. Mater.* **2003**, *15*, 4436.
(16) Velikov, K. P.; Zegers, G. E.; van Blaaderen, A. *Langmuir* **2003**, *19*, 1384.
(17) Zhang, D.; Qi, L.; Ma, J.; Cheng, H. *Adv. Mater.* **2002**, *14*, 1499.
(18) Fukuyo, T.; Imai, H. *J. Cryst. Growth* **2002**, *241*, 193.
(19) Naik, R. R.; Stringer, S. J.; Argarwal, G.; Jones, S. E.; Stone, M. O. *Nat. Mater.* **2002**, *1*, 169.
(20) Walsh, D.; Arcelli, L.; Ikoma, T.; Tanaka, J.; Mann, S. *Nat. Mater.* **2003**, *2*, 386.
(21) Hardikar, V. V.; Matijevic, E. J. *Colloids Surf. A* **2001**, *186*, 23.
(22) Yu, S.; Cölfen, H.; Mastai, Y. *J. Nanosci. Nanotechnol.* **2004**, *4*, 291.
(23) Oaki, Y.; Imai, H. *Cryst. Growth Des.* **2003**, *3*, 711.
(24) He, R.; Qian, X. F.; Yin, J.; Zhu, Z. K. *J. Mater. Chem.* **2002**, *12*, 3783.
(25) Pastoriza-Santos, I.; Liz-Marzan, L. M. *Langmuir* **2002**, *18*, 2888.

CG049823G